Exploitation of host chemokine signalling by pathogenic mycobacteria

Torraca, V.

Chapter 6

The chemokine receptor CXCR4 promotes granuloma formation by sustaining a mycobacteria-induced angiogenesis programme

Vincenzo Torraca, Claudia Tulotta, B. Ewa Snaar-Jagalska and Annemarie H. Meijer

Institute of Biology, Leiden University, The Netherlands

Manuscript in preparation

Chapter 6

The chemokine receptor CXCR4 promotes granuloma formation by sustaining a mycobacteria-induced angiogenesis programme

Vincenzo Torraca, Claudia Tulotta, B. Ewa Snaar-Jagalska and Annemarie H. Meijer

Institute of Biology, Leiden University, The Netherlands

CXC chemokine receptor 4 (CXCR4) plays a critical role in chemotaxis and leukocyte differentiation. Furthermore, there is increasing evidence that links this receptor to angiogenesis. Using the well-established zebrafish-*Mycobacterium marinum* model for tuberculosis, angiogenesis was recently found to be essential to promote the development of cellular aggregates called granulomas that contain the mycobacterial infection and are the hallmark of tuberculosis disease. Here, we found that initiation of the infection-dependent pro-angiogenic programme in mycobacterial disease is dependent on CXCR4 signalling. The nascent granulomas in *cxcr4b*-deficient zebrafish embryos were poorly vascularised, which in turn also delayed bacterial growth in these mutants. Suppressed infection expansion in *cxcr4b* mutants could not be attributed to an overall deficient recruitment of leukocytes or to different intramacrophage bacterial growth rate, as *cxcr4b* mutants displayed similar microbicidal capabilities against initial mycobacterial infection and the cellular composition of granulomatous lesions was similar to wildtype siblings. Expression of *vegfaa* was upregulated to a similar extent in *cxcr4b* mutants and wildtypes, suggesting that the granuloma vascularisation phenotype of *cxcr4b* mutants is independent of vascular endothelial growth factor. However, transcriptional analysis of pro-inflammatory markers (*il1b*, *cxcl18b*) showed that poor vascularisation of the infected tissues in *cxcr4b* mutants is associated with an attenuated inflammatory response. In summary, our study demonstrates that CXCR4-mediated signalling is necessary to induce granuloma-associated angiogenesis and suggests that targeting CXCR4 could provide a potential new anti-angiogenic therapy to suppress the formation of granulomas in TB patients.

GRAPHICAL ABSTRACT

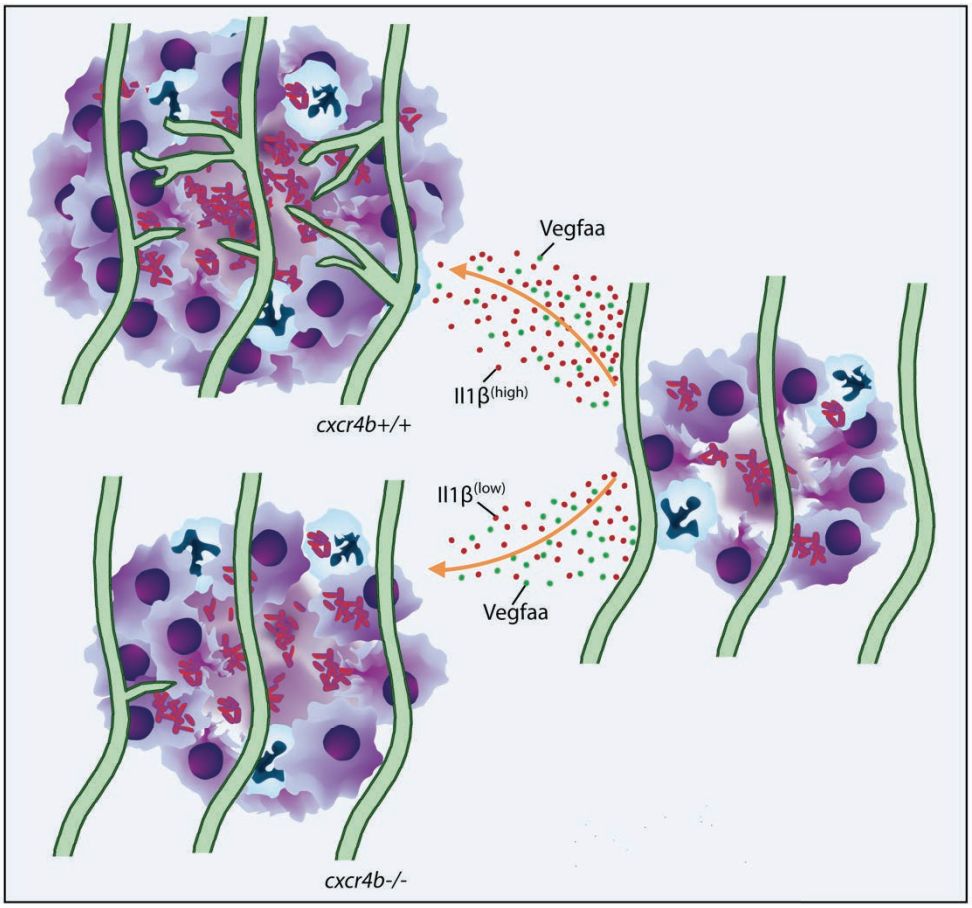

In poorly vascularised tissues, granuloma expansion depends on initiation of an angiogenic programme. Mutation of the chemokine receptor *cxcr4b* can limit the induction of granuloma vascularisation and, in turn, leads to a better containment of bacterial burden. Transcriptional analysis of *cxcr4b* mutants indicates that, while transcription of the main endothelium proliferating factor *vegfaa* remains globally similar in mutants versus wildtypes, *cxcr4b* mutants show reduced induction of the inflammatory mediator *il1b*, which in mammalian systems is known to synergise with VEGF signalling in promoting angiogenesis. Taken together, we propose a model in which blockade of Cxcr4b signalling, via curtailing induction of inflammation limits the initiation of the granuloma vascularisation and therefore the bacterial growth.

INTRODUCTION

CXCR4 is a critical chemokine receptor that controls migration and differentiation of a variety of cell types. In the bone marrow, interaction of CXCR4 with its ligand CXCL12 (SDF1) is required for retention of haematopoietic stem/progenitor cells and their complete differentiation before release into circulation[1,2]. During inflammatory responses, CXCR4 also sustains the trafficking of mature myeloid and lymphoid cells to sites of inflammation. Additionally, CXCR4 signalling on other cells is involved in key migratory mechanisms during development/embryogenesis and CXCR4 has been linked to the metastatic behaviour of cancer cells[3,4,5,6,7,8]. CXCR4 is also well known to play a critical function in HIV pathogenesis, since this factor represents an important HIV co-receptor, mediating viral entry into the host cells[9].

The zebrafish model system has been widely used to study the implication of CXCR4 signalling in different processes. The zebrafish Cxcr4b/Cxcl12a signalling system is implicated in the migration of the primordial germ cells, the lateral line primordium, the migration of haematopoietic stem cells, the recruitment of leukocytes to infectious foci and sites of injury and the invasive movement of cancer cells in tumour metastasis[2,7,10,11,12,13,14]. In other model systems, CXCR4 signalling has also been connected to tumour-sustained angiogenesis[15,16,17]. In particular, CXCR4 stimulation was found to induce expression of vascular endothelial growth factor (VEGF) in human breast carcinoma cells and conversely blockade of CXCR4/CXCL12 signalling was able to suppress tumour angiogenesis and tumour growth *in vivo* in a murine model[15].

Tuberculosis (TB) is caused by *Mycobacterium tuberculosis* (*Mtb*) infection and this disease typically manifests by the formation of aggregates of infected and non-infected immune cells that are known as granulomas. Several studies reported that human tuberculous granulomas are extensively vascularised[18,19,20]. However, very little is understood about the actual relevance of angiogenesis for granuloma formation in TB patients. Additionally, the mechanism by which the vascularisation programme is initiated by the pathogen remains elusive[21,22]. In zebrafish larvae, *Mycobacterium marinum* (*Mm*), a close relative of *Mtb*, causes a disease that recapitulates significant aspects of human TB, which include the formation of necrotising granulomas and the initiation of specific transcriptional and morphological changes in *Mycobacterium*-infected macrophages[23,24]. Using the zebrafish model, it was recently found that *Mm* can also induce granuloma-associated angiogenesis and that initiation of this programme coincides with local induction of hypoxia and of the pro-angiogenic factor *vegfaa*[22]. Notably, the presence of macrophages was strictly necessary for mycobacterial-induced *vegfaa* expression and initiation of granuloma vascularisation. In tumours, activation of CXCR4/CXCL12 signalling is tightly linked to both the development of hypoxia and to the activation of angiogenesis[15,16,17]. Therefore, we hypothesised that this signalling might also affect granuloma vascularisation.

Here we show that Cxcr4b-deficient zebrafish larvae display an attenuated induction of the angiogenic programme at the nascent granulomas. This phenotype was not due to different cellular composition of granulomas, to different chemotaxis of immune cells to the infected areas or to a direct transcriptional control on *vegfaa*, which was still produced in the *cxcr4b* deficient fish, despite the lack of granuloma vascularisation. Our data suggest that *cxcr4b* might be alternatively implicated in pathogenic angiogenesis by controlling the release of

inflammatory pro-angiogenic mediators which maintain a permissive microenvironment that sustains vascularisation. Taken together, our study indicates that Cxcr4b-mediated signalling is required to mediate the full angiogenesis response to mycobacterial infections, and that suppression of pathological angiogenesis with CXCR4 blockers could be explored as an adjuvant treatment of TB patients.

RESULTS

Cxcr4b signalling controls granuloma-induced angiogenesis

To study granuloma-associated angiogenesis, a trunk infection model was recently established in zebrafish embryos (**Figure 1A-B**). In this model a transgenic *Tg(kdrl:eGFP)* background (labelling arterial and venous endothelium) was used to monitor host vascularisation in the environment of the nascent granulomatous lesions (**Figure 1C-E**) [22,25]. To study whether *cxcr4b* has a function in granuloma vascularisation, we injected mCherry-fluorescent *Mm* in *cxcr4b* mutant and wildtype (wt) siblings at 2 days post fertilisation (dpf) and measured bacterial expansion and vascularisation of the infected area at 5 days post infection (dpi) (**Figure 1F-K**).

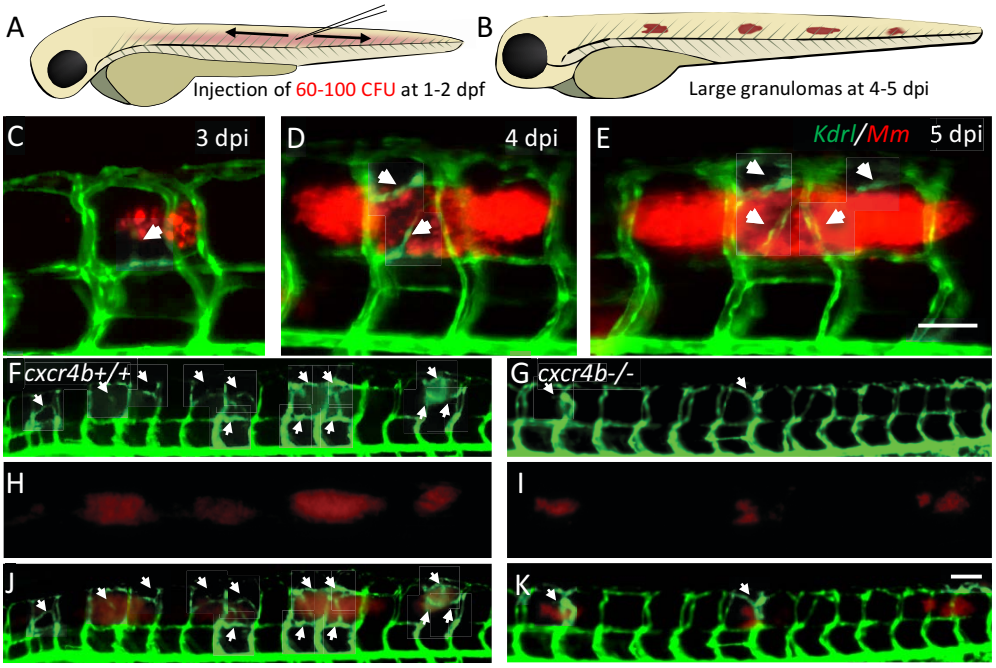

Figure 1. Trunk granuloma formation and induction of angiogenesis by *M. marinum*. A-B. Schematic representation of injection location and of granuloma expansion in zebrafish embryos/larvae upon injection of *Mm* into the trunk. **C-E.** Longitudinal imaging of vascular and bacterial growth during development of a trunk granuloma in the *Tg(kdrl:eGFP)* line at 3, 4 and 5 dpi. **F-K.** Formation of trunk granulomas and their vascularisation in a *cxcr4b*$^{+/+}$ and *cxcr4b*$^{-/-}$ larva at 5 dpi. White arrows indicate sites of abnormal vascularisation associated to bacterial growth, notably largely initiated in the wt but rare in the mutant. Scale bars: 100 µm.

In *cxcr4b*$^{-/-}$ larvae, the expansion of the infection progressed at a significantly lower rate as compared to the lesions in wt (**Figure 1F-K)**. Simultaneously, the association of vascularisation with the granulomas was impaired in these mutants and, differently from wt, *cxcr4b* mutants did not have a significant positive correlation between granuloma size and length of associated abnormal vasculature (**Figure 2A-C**). Corroborating these results, even large granulomas failed vascularisation in *cxcr4b*$^{-/-}$ (**Figure 2D-I**).

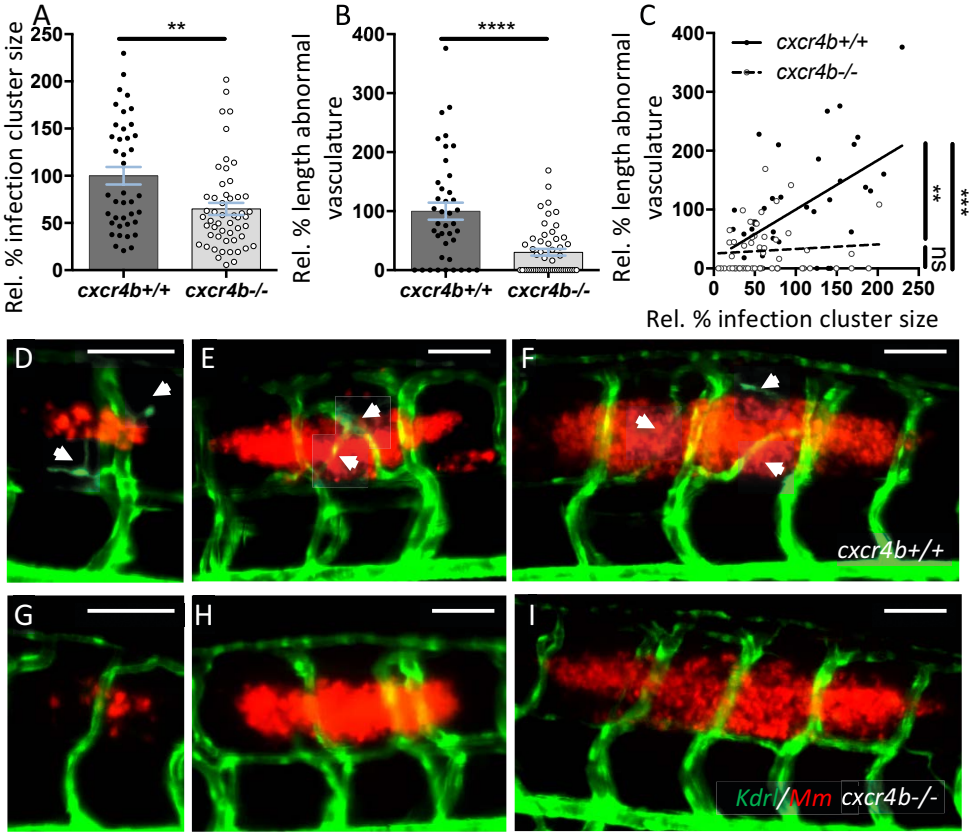

Figure 2. Cxcr4b mutation impairs granuloma-induced angiogenesis. A-B. *cxcr4b* mutants display a reduced expansion rate of local granulomatous lesions (A), which coincided with the incapability to induce an angiogenic programme (B). **C**. Vascularisation/granuloma expansion correlation analysis. In wt, the expansion of the granulomas depends on the activation of the angiogenetic programme at the infection focus. Differently, in *cxcr4b* mutants, no significant correlation between granuloma size and vessel length could be observed and even large granulomas failed to initiate angiogenesis, suggesting that the differential activation of the angiogenic programme is not the effect, rather the cause, of reduced burden in mutants. Data points refer to individual trunk granulomas at 5 dpi (3 replicates cumulated). Values are expressed in % relative to average wt (set to 100%). Significance in C indicates that the slopes of *cxcr4b*$^{-/-}$ and *cxcr4b*$^{+/+}$ trend lines are different and that in wt (but not in mutants) this slope is different from 0 (*x* axis). **D-I.** Representative images of comparably-sized 5 dpi trunk granulomas in *cxcr4b*$^{-/-}$ and *cxcr4b*$^{+/+}$, notably *cxcr4b*$^{-/-}$ granulomas display a defect in local vascularisation, which is independent of the granuloma size. Scale bars: 100 µm.

The interdependence between granuloma expansion and angiogenesis had been previously described[22] and mechanistically resembles closely the angiogenic switch in tumorigenesis, in which tumour size is directly related to the local induction of pathogenic vascularisation[26]. Altogether, our findings suggest that *cxcr4b* mutation affects granuloma expansion by primarily affecting the initiation of the angiogenesis programme, and the difference in infection burden appears to be the consequence, rather than the cause, of impaired angiogenetic support of granuloma formation.

cxcr4b mutation does not alter the migratory and microbicidal capabilities of macrophages or the cellular composition of the granulomatous lesions

Since others had previously found that intramacrophage residence of mycobacteria is indispensable for initiation of angiogenesis[22], we investigated whether the difference in promotion of angiogenesis in *cxcr4b* mutants could be explained by aberrant macrophage recruitment (and therefore different intracellular/extracellular ratios), differential microbicidal capability of macrophages, or alteration in the macrophage composition of granulomatous lesions. When mycobacteria were injected locally into the hindbrain ventricle, a comparable number of leukocytes were promptly recruited (3 hpi) to the infected site in mutants and wt (**Figure 3A-B**). To assess the possibility of an altered microbicidal capability, we injected the *Mm* mutant strain *Δerp*, which is highly susceptible to macrophage clearance and replicates intracellularly at a low rate, thereby permitting quantification of mycobacterial growth in individual macrophages by live microscopy. At 44 hpi the percentage of macrophages displaying low (1-5 bacteria), moderate (6-10 bacteria) or high (>10 bacteria) infection load was quantified and *cxcr4b* mutants showed similar distribution of the infection phenotypes as wt siblings, indicating that depletion of *cxcr4b* does not alter the macrophages capability to counteract intracellular infection (**Figure 3C-D**). That *cxcr4b* mutation might affect the content of macrophages in the mature granulomas was also excluded, as the percentage of mycobacteria co-localising with macrophages was similar in mutant and wt siblings (**Figure 3E-G**). In zebrafish larvae, *cxcr4b* is expressed both by the macrophage lineage (marked by *mpeg1*) and by the neutrophil lineage (marked by *mpx*) (**Figure 3H**). However, it is unlikely that the angiogenesis deficiency in *cxcr4b* mutants depended on *cxcr4b* expression by neutrophils, as suggested by *irf8* morpholino knockdown, which skews myelopoiesis towards neutropoiesis at the expense of primitive macrophage development (**Figure 3I-J**)[27]. In this situation the initial deficiency in macrophages was already sufficient to abrogate the angiogenetic response, indicating that neutrophils alone cannot support angiogenesis and therefore that the *cxcr4b* mutation phenotype implicates a macrophage-related function. However, since recruitment of macrophages, cellular composition of lesions and intramacrophage killing of bacteria were comparable between mutants and wt (**Figure 3**), we hypothesised that *cxcr4b* mainly affects the interaction of the macrophages with the surrounding tissue.

The granuloma vascularisation defect in _cxcr4b_ mutants associated with reduced inflammatory gene expression

Since CXCR4 was previously linked to tumour angiogenesis via a transcriptional control on VEGF signalling[15], we addressed whether *cxcr4b* mutation controlled granuloma angiogenesis by affecting Vegf signalling.

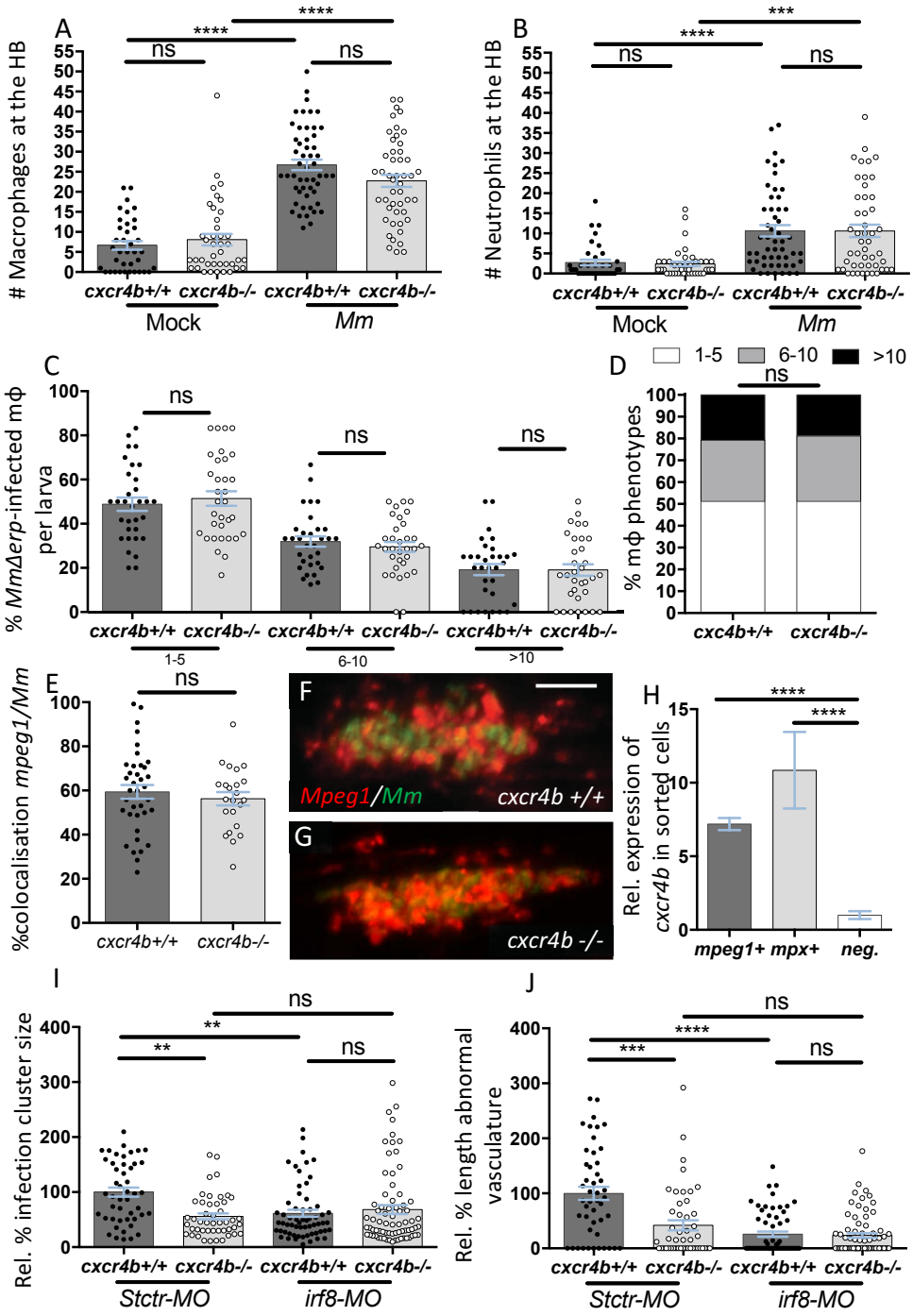

Figure 3. ***cxcr4b*** **is not required for the establishment of macrophage parasitism, but macrophages are necessary to mediate** ***cxcr4b*****-dependent angiogenesis** *(Legend on the next page)*.

Figure 3. *cxcr4b* is not required for the establishment of macrophage parasitism, but macrophages are necessary to mediate *cxcr4b*-dependent angiogenesis *(Figure on the previous page).* **A-B.** Recruitment of macrophages (A) and neutrophils (B) 3 hours post local hindbrain (HB) infection at 2 dpf with *Mm* was unaffected by *cxcr4b* mutation. Each value represents the recruitment measured in 1 embryo (2 replicates, cumulated). **C-D.** *cxcr4b* is dispensable for the capability of macrophages to counteract intracellular replication of *Mm Δerp.* Infected macrophages (*mpeg1:mCherry-F*$^{+}$) were classified into three phenotypic classes, according to the severity of intracellular infection (1-5, 6-10, or >10 bacteria). C represents the % of macrophages per larva that populates each class. D represents the overall distribution of macrophage phenotypes (macrophages from all larvae cumulated). Graphs are cumulated from 2 independent replicates. **E-G.** % of *mpeg1:mCherry-F* signal overlapping with *Mm-GFP* signal in *cxcr4b*$^{-/-}$ and *cxcr4b*$^{+/+}$. No significant deviation in macrophage composition of the trunk granuloma lesions was detected. Each data point represents 1 lesion (1 replicate). Representative example images are shown in F and G. **H.** Expression of *cxcr4b* in macrophages (*mpeg1*$^{+}$) and neutrophils (*mpx*$^{+}$). Both cell subsets express *cxcr4b* at significantly higher levels than the negative (non-fluorescent) cell population. Data represent fold changes relative to the negative cell fraction. Cells were sorted at 2 dpf (3 replicates). **I-J.** Macrophages are indispensable to mediate granuloma vascularisation (I) and an increased number of neutrophils (by *irf8* morpholino knockdown) cannot compensate for macrophage deficiency, neither in *cxcr4b*$^{-/-}$ nor in *cxcr4b*$^{+/+}$. Deficient bacterial expansion in *irf8* knockdown condition (*irf8-MO*) compared to standard control morpholino treatment (*Stctr-MO*) can be attributed to the lack of vascularisation as suggested by non-significant differences in burden between the knockdowns and control *cxcr4b*$^{-/-}$ (J). Data are analysed as in Figure 2A-B, but infections were performed at 33 hpf, instead of 2 dpf (1 replicate).

Treatment with Sunitinib (a Vegf receptors inhibitor)[28] or *cxcr4b* mutation reduced trunk granuloma size to the same level (**Figure 4A**), although Vegf receptor inhibition could still synergise with *cxcr4b* mutation and could more severely suppress granuloma vascularisation (**Figure 4B**). However, it should be noted that treatment with Sunitinib (but not *cxcr4b* mutation) also affected to some extent physiological angiogenesis, as the frequency of physiological sprouting from intersegmental vessels and their lateral fusion was also reduced by this treatment (not shown). Since the angiogenesis response to mycobacterial infection was found to coincide with local induction of *vegfaa*[22] and since mammalian CXCR4 has been linked to a transcriptional regulation of *VEGFA*[15], we addressed whether *cxcr4b* affected angiogenesis by exerting a similar transcriptional control on *vegfaa* expression in our model. Whole mount qRT-PCR analysis revealed that both mutants and wt upregulated *vegfaa* to a comparable level (**Figure 4C**). We also found that the levels of *vegfaa* induction, although significant, were limited (1.5-fold) when compared to the induction of other infection-inducible genes, which could be seen highly upregulated in the same conditions (**Figure 4C**). Likewise, expression of *cxcl12a* (encoding the ligand of Cxcr4b) showed limited but comparable induction in mutants and wt (**Figure 4C**). Expression of *Cxcr4b* mRNA was not relevantly altered by the infection and remained comparable between *wt* and mutants (the *cxcr4b* mutant mRNA differs from the wt only because of a point mutation and can, therefore, be normally tested by qRT-PCR). Signalling via CXCR4 has been linked to the induction of inflammatory genes during the response to infections[29,30] and the local chronic induction of inflammation mediators is known to play a critical role to sustain vascularisation of damaged/inflamed tissues[31,32]. Several inflammatory molecules (mainly interleukins IL1β-6-8 and TNFα) have been largely connected to the sustenance of pathological vascularisation in inflammatory diseases[32,33].

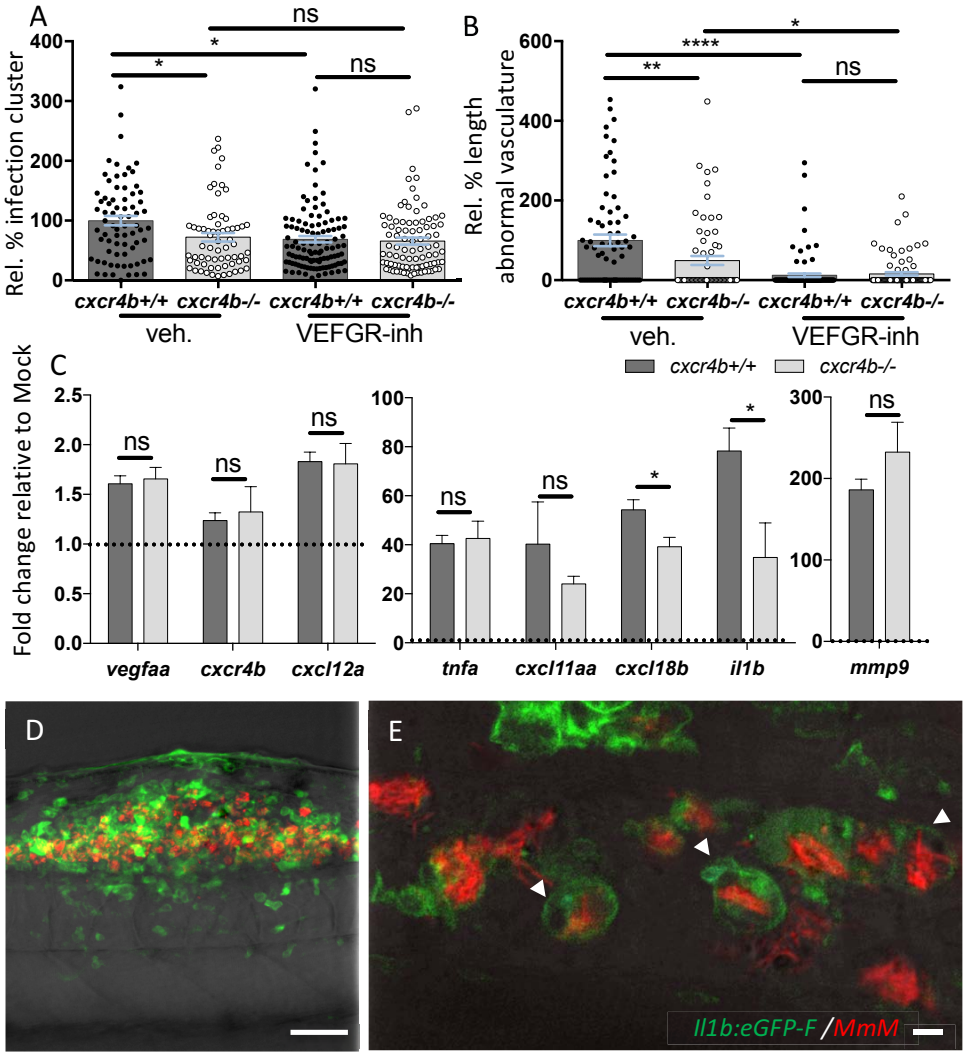

Figure 4. *cxcr4b* mutation does not affect *vegfaa* expression but attenuates expression of inflammatory genes. **A-B.** Cxcr4b deficiency reduced granuloma expansion to a similar extent as blockade of Vegf signalling (VEGFR-inh, treatment with Sunitinib) (A), although Vegf inhibition can more severely affect angiogenesis. (B). Data are analysed as in Figure 2A-B (2 replicates, cumulated). **C**. At 5 dpi, Cxcr4b does not exert a transcriptional control on *vegfaa* expression, but affects the inflammatory response to mycobacterial infection. qRT-PCR were performed whole mount from pools of at least 10 embryos (4 replicates). Data represent fold changes of *Mm* infection groups relative to their mock injection (2% PVP in PBS) control group (set to 1, dotted line). No significant differences in basal expression levels were found between mutants and wt for the analysed genes. **D-E.** Induction of the pro-angiogenetic inflammatory mediator *il1b* at the trunk granuloma. The large granuloma forming in the trunk contains a high number of *il1b*-expressing cells, predominantly consisting of infected cells. Confocal images were acquired at 5 dpi from infected *Tg(il1b:eGFP-F)* larvae. Scale bars: D: 50 µm; E: 5 µm.

In agreement, the use of the transgenic reporter *Tg(il1b:eGFP-F)*[34] revealed high expression of *il1b* by *Mm*-infected cells composing the granulomatous lesions in zebrafish larvae (**Figure 4D-E**). Therefore, we analysed the expression profile of *il1b* and several other *Mm*-inducible inflammatory genes (*tnfa*, *cxcl11aa*, *cxcl18b* and *mmp9*). All these genes could be still induced in *cxcr4b* mutants. However, two of the analysed genes, namely *cxcl18b* and *il1b* were significantly less induced in the mutants, when compared to wt (**Figure 4C**). Taken together, this suggests that a differential inflammatory response can be elicited in *cxcr4b* mutants and wt during the infection progression.

DISCUSSION

Using intravital imaging in the zebrafish–*Mm* infection model, we have investigated the function of the homoeostatic chemokine receptor Cxcr4 in the development of mycobacterial infection and granuloma formation. We found that zebrafish embryos/larvae carrying a homozygote mutation of *cxcr4b* developed an attenuated disease which could be associated with the inability of these mutants to induce local angiogenesis. Supporting that Cxcr4b promotes granuloma formation by sustaining a mycobacteria-induced angiogenesis programme, the positive correlation between granuloma growth and vascularisation that is normally observed in wt larvae, was lost in *cxcr4b* mutants. Furthermore, pharmacological blockade of the angiogenesis programme by Vegfr inhibitor could fully abolish the differences between mutants and wt in the exacerbation of mycobacterial infection. The use of angiogenesis inhibitors has previously been proposed as a host-targeted therapy to suppress the formation of granulomas in TB patients[22]. Based on our results, the CXCR4 receptor could be explored as a novel target for anti-angiogenic tuberculosis therapy.

It is unlikely that the granuloma vascularisation phenotype requires expression of *cxcr4b* by the endothelial cells *per se*, since several studies have identified that venous/arterial endothelium (*kdrl*$^{+}$) does not express high levels of *cxcr4b* and that this gene can be found expressed only in sporadic sprouting lymphatic vessels (*kdrl*$^{-}$)[12,35]. Although our own transcriptional analysis of FACS-sorted *kdrl*$^{+}$ cells at 5 dpi revealed that transcript of *cxcr4b* can be detected in these cells, this gene is more abundantly expressed by the macrophage (*mpeg1*$^{+}$) fraction (**Supplementary Figure 1**). Our study suggests that *cxcr4b* function in evoking angiogenesis requires the presence of macrophages, since skewing haematopoiesis towards neutrophils at the expenses of macrophages severely affected the induction of the angiogenesis. This conclusion is in line with previous data showing that macrophage depletion by transcription factor *spi1/pu.1* knockdown reduced the recruitment of new vessels to the *Mm* infection foci[22]. Together, these results support that *cxcr4b* exerts its function on macrophages in a cell-autonomous fashion, and affects their capability to promote angiogenesis.

Macrophages of *cxcr4b* mutants were normally capable of migrating to initial mycobacterial infection foci and were equally suited to contain initial intramacrophage bacterial replication, therefore excluding significant effects of *cxcr4b* on the establishment of mycobacteria/macrophage parasitism. Apart from the deficiency in the expansion rate and the absence of associated vascularisation, infectious lesions of *cxcr4b*$^{-/-}$ were structurally undistinguishable from those of wt when granulomas of similar sizes were compared. Since previous studies reported that *vegfaa* expression pattern coincided with the local promotion of granuloma angiogenesis[22], we hypothesised that Cxcr4b might support angiogenesis via promotion of *vegfaa* expression. The induction levels of *vegfaa* in

Mm infected larvae were low and we could not detect a significant difference between infected *cxcr4b* mutants and wt. Several studies have shown that VEGF induction in inflammatory processes can be transient and largely variable[36,37,38]. Therefore, a direct function of *cxcr4b* in the regulation of Vegf/Vegfr signalling cannot be completely excluded by our study. Interestingly, we observed a more pronounced effect of *cxcr4b* mutation on the induction of inflammatory mediators, especially *ilb* and *cxcl18b*. Several reports showed that CXCR4 signalling can support inflammation. In particular, elegant studies revealed that CXCR4 can cross-talk with the plasma membrane Toll-like receptor TLR4 and act as a potent co-stimulatory mediator[29,30]. This leads us to hypothesise that *cxcr4b* may contribute to the maintenance of a favourable pro-angiogenesis microenvironment, by sustaining the production of inflammatory factors.

There is growing evidence of a tight link between the angiogenesis process and inflammation[31,32]. Many factors that are produced to promote the inflammatory response can also promote angiogenesis. Inflammatory cells, especially macrophages, are exceptional producers of these pro-angiogenic mediators, which include prostaglandins, TNFα, interleukins (especially IL1β-6-8)[31,32,33]. IL8/CXCL8 is both chemotactic and mitogenic for endothelial cells[39,40]. Similarly, IL1β has been reported to be a potent inducer of endothelial cell migration and proliferation, which induces profound morphological transformations of these cells and changes in the expression profile, including induction of genes that are intimately involved in the regulation of blood vessel formation[33,41,42]. A transcriptional analysis of endothelial cells upon stimulation with either VEGF or IL1 reported about 80% overlap of their transcriptional signature, which coincided with a cluster of core pro-angiogenetic genes involved in cell proliferation, chemotaxis and blood vessel differentiation[43]. In a matrigel model for angiogenesis, both IL1β and VEGF signalling were indispensable and neutralisation of either one of these factors was sufficient to fully abolish the angiogenic response[33,42].

In our study Il1β, which was significantly suppressed at transcriptional levels in infected *cxcr4b* mutants compared to infected wt larvae, may represent a key impaired pro-angiogenetic mediator. Additionally, Cxcl18b, a fish specific chemokine, appeared also significantly downregulated in these mutants. Despite that the role of this chemokine has not been fully elucidated, our own studies indicate that this chemokine shares high functional similarities with IL8/CXCL8[44], indicating that, similarly to IL8/CXCL8, Cxcl18b might also be important for chemotaxis and cell division of the endothelial cells. The importance of inflammation for granuloma vascularisation in the zebrafish trunk-granuloma model is also suggested by previous studies, where attenuated (ESX1-deficient) *Mm* could not induce angiogenesis even when larvae were injected with larger inoculums to compensate for the infection burden difference[22]. Similarly, also non-chronic infections (*E. coli*) did not evoke the angiogenetic programme[22]. Whether *cxcr4b* sustains activation of the angiogenic programme by supporting the release of inflammatory mediators that are chemotactic/mitogenic for the endothelial cells will require additional characterisation and the zebrafish model may represent an elective surrogate system to further address the angiogenesis/inflammation co-dependency *in vivo*.

Concluding, the angiogenesis programme mounted at the granuloma is important to sustain the further expansion of the lesion and is a complex multifaceted process that involves pathogen virulence factors, macrophage response to intracellular infection and granuloma aggregation, induction of local hypoxia and *vegfaa* signalling[22]. Our addition to this

scenario is that the homoeostatic chemokine receptor CXCR4 is critical to permit the induction of the angiogenetic programme, a mechanism that could be exerted by modulation of the inflammatory pro-angiogenetic mediators released in the granuloma microenvironment, such as IL1β. Manipulation of the inflammation/angiogenesis interface triggers significant consequences to the pathology of the mycobacterial infection and interfering with this programme via host-directed therapies can be useful to limit mycobacterial disease. This and previous studies have shown that similar suppression of mycobacterial growth can be obtained by directly blocking VEGF/VEGFR signalling or by limiting the inflammatory response[22,23,45,46,47]. However, blockade of CXCR4 may provide a preferential treatment, for example in HIV-positive TB patients, where CXCR4 plays also a relevant function in viral entry, therefore, its suppression would simultaneously counteract both mycobacterial and viral infection.

MATERIALS AND METHODS

Zebrafish lines and maintenance – Zebrafish lines were handled in compliance with the local animal welfare regulations and maintained according to standard protocols (zfin.org). The study was approved by the local animal welfare committee (DEC) of the University of Leiden (licence number: 10612). Fish lines used in this work were the following: wildtype strain AB/TL, *Tg(il1b:eGFP-F^{zf550})*[34] the double transgenic line *Tg(mpeg1:mCherry-F^{ump2}/mpx:eGFP^{i114})*[48,49], *cxcr4b* homozygote mutant (*cxcr4b*$^{-/-}$) and wildtype (*cxcr4b*$^{+/+}$) siblings of *(cxcr4b^{t26035})*[8,14] crossed into the transgenic backgrounds of *Tg(kdrl:eGFP^{s843})*[25] or *Tg(mpeg1:mCherry-F^{ump2})*. Embryos were grown at 28.5°C in egg water (60 µg/ml sea salt, Sera Marin, Heinsberg, Germany). Larvae destined to image acquisition were maintained in egg water supplemented with 0.003% PTU (1-phenyl-2-thiourea, Sigma-Aldrich, St Louis, MO, USA) from 8-12 hpf to prevent melanisation. Anaesthesia of embryos/larvae used for live imaging was achieved with 0.02% buffered Tricaine (3-aminobenzoic acid ethyl ester, Sigma-Aldrich) in egg water.

Bacterial cultures and infection delivery – Approximately 60-100 CFU suspended in a volume of 10 nl of *M. marinum* strain M (or where specified its isogenic mutant strain *Δerp*) constitutively expressing mCherry, eGFP or Wasabi[50,51] were injected into the trunk at 2 dpf[22], while approximately 50 CFU in a volume of 1 nl were injected into the hindbrain (HB, 2 dpf). For recruitment assays and qRT-PCR experiments, the same volume of mock [2% polyvinylpyrrolidone-40 (Sigma-Aldrich) in phosphate buffer saline (PBS)] was injected in control embryos, as a reference control. Bacteria were grown and harvested from an O/N culture as described previously[52,53]. For morpholino experiments (*irf8* knockdown) and collection of samples for qRT-PCR, trunk infections were performed at 33 hpf (instead of 2 dpf). For the assessment of the microbicidal activity of macrophages against initial mycobacterial infection, single cell suspensions of *Mm Δerp*-mWasabi were injected into the caudal vein at 33 hpf from -80ºC frozen single-use aliquots, using a protocol adapted from reference[51]. Briefly, bacteria from a 1-week-old plate were inoculated to an OD600 of 0.2 in 10 ml 7H9 medium supplemented with ADC enrichment. The culture was grown for 24 h to reach an OD of approximately 1.0. Bacteria were washed 3 times with PBS and suspended in PBS supplemented with 10% glycerol to an OD600 of 5.0. To generate a single cell suspension, bacteria were passed 10 times through a syringe. 50 µl aliquots were frozen in liquid nitrogen and stored at -80ºC. Upon thawing, the vital bacteria were quantified by plating as being approximately 100 CFU/nl. For quantification of macrophage and neutrophils recruitment to mycobacteria, 2 dpf embryos

were infected in the hindbrain, fixed at 3 hpi in 4% paraformaldehyde in PBS supplemented with 0.08% Triton X-100 and prepared for combined L-plastin (Lp) immunostaining and myeloperoxidase (Mpx) enzymatic activity staining as in reference[54]. Leukocytes accumulated at the injected cavity (macrophages: Lp-positive and Mpx-negative; neutrophils: Mpx-positive) were counted using a Leica MZ16FA fluorescence stereomicroscope (Leica Microsystems, Rijswijk, The Netherlands).

RNA isolation, FACS and qRT-PCR – To evaluate the induction of genes upon infections (**Figure 4C**), whole-embryo RNA extraction, cDNA synthesis and qRT-PCR were performed at 5 dpi from a pool of embryos injected at 33 hpi (4 replicates), according to the procedure described in reference[52]. To demonstrate expression by phagocytes (**Figure 3H**), RNA was isolated from *mpx*$^{+}$ and *mpeg1*$^{+}$ cells sorted at 2 dpf from the double transgenic line *Tg(mpeg1:mCherry-F*^{ump2}*/mpx:eGFP*^{i114}*),* according to previous reports[55,52]. Similarly, to evaluate expression of *cxcr4b* by endothelial cells (**Supplementary Figure 1**), RNA was isolated from *kdrl*$^{+}$ or *mpeg*1^{+} cells of *cxcr4b*$^{+/+}$ and *cxcr4b*$^{-/-}$ larvae (5 dpi/6 dpf) derived from paired crosses of *Tg(mpeg1:mCherry-F/cxcr4b*$^{+/+}$*)* x *Tg(kdrl:eGFP/cxcr4b*$^{+/+}$*)* and *Tg(mpeg1:mCherry-F/cxcr4b*$^{-/-}$*)* x *Tg(kdrl:eGFP/cxcr4b*$^{-/-}$*)*.

Reference housekeeping genes were *ppia1b* for whole-mount samples and *eif4a1b* for FACS-sorted samples. qRT-PCR primers are reported in **Supplementary Table S1**.

Pharmacological inhibition of VEGF signalling – For pharmacological inhibition of VEGF signalling, the VEGFR tyrosine kinase inhibitor Sunitinib (1 µM, Sigma-Aldrich) or vehicle treatment (0.1% DMSO, Sigma-Aldrich), were applied directly to the egg water and refreshed every 2 days according to reference[28].

***Irf8* knockdown** – 1 nl of 1 mM *irf8* splicing morpholino (5′-AATGTTTCGCTTACTTTGAAAATGG-3′, Gene tools)[27] or the same concentration of a standard control morpholino (5′-CCTCTTACCTCAGTTACAATTTATA-3′, Gene tools) were injected in one-cell stage zebrafish fertilised eggs according to reference[27].

Imaging and image quantification – Fixed or live embryos and larvae were imaged using a Leica MZ16FA fluorescence stereomicroscope. The size of individual granulomas was quantified at 5 dpi (at 4 dpi in case of *irf8* morpholino knockdown) by pixel count, using Fiji/ImageJ software (NIH, Bethesda, MD, USA) according to reference[52]. The length of abnormal vasculature at the granulomas was quantified at the same stage from images according to reference[22]. To score the microbicidal activity of macrophages against mycobacteria, *MmΔerp*-Wasabi bacteria prepared as described above were injected into the caudal vein of *Tg(mpeg1:mCherry-F)/cxcr4b*$^{-/-}$ and *Tg(mpeg1:mCherry-F)/cxcr4b*$^{+/+}$ embryos. Intramacrophage mycobacterial sites of growth were counted (blind) from fixed embryos at 44 hpi according to reference[47] , using Zeiss Observer 6.5.32 confocal microscope and a C-Apochromat 63x/1.20 W Korr UV-VIR-IR M27 objective (Carl Zeiss, Sliedrecht, The Netherlands). The level of infection per macrophage was classified into three groups based on bacterial content (1-5 bacteria, 6-10 bacteria or >10 bacteria). To estimate similar macrophage content of granulomas, the percentage of colocalisation of *Tg(mpeg1:mCherry-F)* and *Mm* M-eGFP was quantified ad 5 dpi using Fiji/ImageJ dedicated colocalisation plugin. Confocal images in **Figure 4** were taken from trunk granulomas at 5 dpi/6 dpf, using Zeiss Observer 6.5.32 confocal microscope and an EC

Plan-Neofluar 20x/0.50 M27 (**Figure 4D**) or C-Apochromat 63x/1.20 W Korr UV-VIR-IR M27 objective (**Figure 4E**).

Statistical analysis – Statistical significance was analysed using GraphPad Prism 6 (GraphPad Software, La Jolla, CA, USA). Differences in granuloma sizes, angiogenesis, recruitment and bacteria/macrophage co-localisation were statistically tested by Mann-Whitney test (comparison between 2 groups) or Kruskal-Wallis test followed by Šidák comparison test (multiple group comparisons) (**Figure 2A-B**, **Figure 3A-B-E**, **Figure 4A-B**). Bacterial cluster size/angiogenesis correlation (**Figure 2C**) was analysed by Pearson correlation test and the difference between mutant and wt regressions was computed by GraphPad Prism 6 dedicated linear regression analysis tool. No differences in bacterial replication and in the distribution of macrophages in the three phenotypic classes (as defined above) were analysed by two-tailed *t*-tests per each phenotypic class (**Figure 3C**) and by chi-square contingency test (**Figure 3D**) respectively. For qRT-PCR (**Figure 4C**), statistical significance was estimated by two-tailed *t*-tests on ln(n)-transformed relative induction folds. Significance (*P*-value) is indicated with: ns, non-significant; **P*<0.05; ***P*<0.01; ****P*<0.001, *****P*<0.0001. Error bars: mean±s.e.m.

ACKNOWLEDGEMENTS

We thank Georges Lutfalla for having provided the *Tg(il1b:eGFP-F)* transgenic line.

This work was supported by the European Marie-Curie Initial Training Network FishForPharma (contract number PITN-GA-2011-289209) and by the Netherlands Organisation for Scientific Research (TOP GO Grant: 854.10.012).

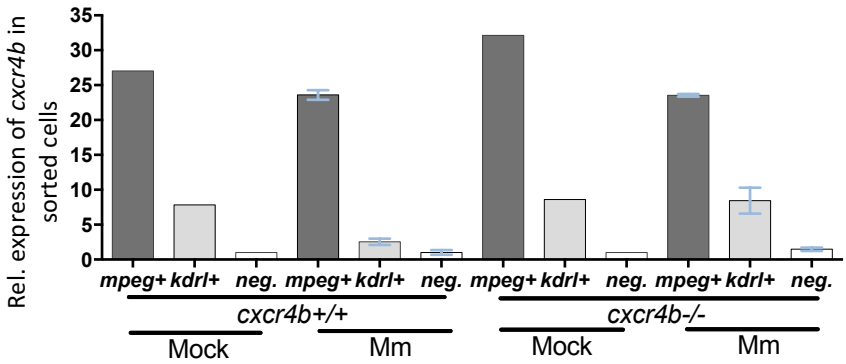

Supplementary Figure 1. Expression levels of *cxcr4b* in FACS-sorted macrophages and endothelial cells during mycobacterial infection. Data represent fold changes relative to the negative cell population. Cells were sorted at 5 dpi (2 replicates for *Mm* infected groups and 1 replicate for mock control) from pools of embryos injected at 33 hpf.

Gene	Transcript reference	qRT-PCR Fw (5'-3')	qRT-PCR Rv (5'-3')	Ref.
vegfaa	ENSDART00000167719	TGCTCCTGCAAATTCACACAA	ATCTTGGCTTTTCACATCTGCAA	Li *et al.* 2012
cxcr4b	ENSDART00000061499	GCGACCTCTCAGTCAGCAAT	TCACAAGCACCACAAGTCCA	-
cxcl12a	ENSDART00000053946	GCTGGTGCCGTTCCACAGTCA	GGGGCAGTTGGGTGTGTGGAG	-
tnfa	ENSDART00000025847	AGACCTTAGACTGGAGAGATGAC	CAAAGACACCTGGCTGTAGAC	Stockhammer *et al.* 2009
cxcl11aa	ENSDART00000169606	ACTCAACATGGTGAAGCCAGTGCT	CTTCAGCGTGGCTATGACTTCCAT	Torraca *et al.* 2015
cxcl18b	ENSDART00000111598	TCTTCTGCTGCTGCTTGCGGT	GGTGTCCCTGCGAGCACGAT	Van der Vaart *et al.* 2013
il1b	ENSDART00000169225	GAACAGAATGAAGCACATCAAACC	ACGGCACTGAATCCACCAC	Stockhammer *et al.* 2009
mmp9	ENSDART00000062845	CATTAAAGATGCCCTGATGTATCCC	AGTGGTGGTCCGTGGTTGAG	Stockhammer *et al.* 2009
ppiab	ENSDART00000166085	ACACTGAAACACGGAGGCAAAG	CATCCACAACCTTCCCGAACAC	Stockhammer *et al.* 2009
eif4a1b	ENSDART00000140602 ENSDART00000011878	TTCAGAAACTCAGTACTAGCATACA	GTGACATCCAACACCTCTGC	Benard *et al.* 2015

Supplementary Table 1. Primers used for qRT-PCR in this study.

REFERENCES

1 Furze RC, Rankin SM. Neutrophil mobilization and clearance in the bone marrow. Immunology. 2008 Nov;125(3):281-8.

2 Walters KB, Green JM, Surfus JC, Yoo SK, Huttenlocher A. Live imaging of neutrophil motility in a zebrafish model of WHIM syndrome. Blood. 2010 Oct 14;116(15):2803-11.

3 Fricker SP. A novel CXCR4 antagonist for hematopoietic stem cell mobilization. Expert Opin Investig Drugs. 2008 Nov;17(11):1749-60.

4 Uy GL, Rettig MP, Cashen AF. Plerixafor, a CXCR4 antagonist for the mobilization of hematopoietic stem cells. Expert Opin Biol Ther. 2008 Nov;8(11):1797-804.

5 Doitsidou M, Reichman-Fried M, Stebler J, Köprunner M, Dörries J, Meyer D, Esguerra CV, Leung T, Raz E. Guidance of primordial germ cell migration by the chemokine SDF-1. Cell. 2002 Nov 27;111(5):647-59.

6 Gelmini S, Mangoni M, Serio M, Romagnani P, Lazzeri E. The critical role of SDF-1/CXCR4 axis in cancer and cancer stem cells metastasis. J Endocrinol Invest. 2008 Sep;31(9):809-19.

7 Mukherjee S, Manna A, Bhattacharjee P, Mazumdar M, Saha S, Chakraborty S, Guha D, Adhikary A, Jana D, Gorain M, Mukherjee SA, Kundu GC, Sarkar DK, Das T. Non-migratory tumorigenic intrinsic cancer stem cells ensure breast cancer metastasis by generation of CXCR4(+) migrating cancer stem cells. Oncogene. 2016 Feb 29.

8 Tulotta C, Stefanescu C, Beletkaia E, Bussmann J, Tarbashevich K, Schmidt T, Snaar-Jagalska BE. Inhibition of signaling between human CXCR4 and zebrafish ligands by the small molecule IT1t impairs the formation of triple-negative breast cancer early metastases in a zebrafish xenograft model. Dis Model Mech. 2016 Feb 1;9(2):141-53.

9 Alkhatib G, Berger EA. HIV coreceptors: from discovery and designation to new paradigms and promise. Eur J Med Res. 2007 Oct 15;12(9):375-84.

10 Donà E, Barry JD, Valentin G, Quirin C, Khmelinskii A, Kunze A, Durdu S, Newton LR, Fernandez-Minan A, Huber W, Knop M, Gilmour D. Directional tissue migration through a self-generated chemokine gradient. Nature. 2013 Nov 14;503(7475):285-9.

11 Haas P, Gilmour D. Chemokine signaling mediates self-organizing tissue migration in the zebrafish lateral line. Dev Cell. 2006 May;10(5):673-80.

12 Tamplin OJ, Durand EM, Carr LA, Childs SJ, Hagedorn EJ, Li P, Yzaguirre AD, Speck NA, Zon LI. Hematopoietic stem cell arrival triggers dynamic remodeling of the perivascular niche. Cell. 2015 Jan 15;160(1-2):241-52.

13 Raz E, Mahabaleshwar H. Chemokine signaling in embryonic cell migration: a fisheye view. Development. 2009 Apr;136(8):1223-9.
14 Knaut H, Werz C, Geisler R, Nüsslein-Volhard C; Tübingen 2000 Screen Consortium. A zebrafish homologue of the chemokine receptor Cxcr4 is a germ-cell guidance receptor. Nature. 2003 Jan 16;421(6920):279-82.
15 Liang Z, Brooks J, Willard M, Liang K, Yoon Y, Kang S, Shim H. CXCR4/CXCL12 axis promotes VEGF-mediated tumor angiogenesis through Akt signaling pathway. Biochem Biophys Res Commun. 2007 Aug 3;359(3):716-22.
16 Massena S, Christoffersson G, Vågesjö E, Seignez C, Gustafsson K, Binet F, Herrera Hidalgo C, Giraud A, Lomei J, Weström S, Shibuya M, Claesson-Welsh L, Gerwins P, Welsh M, Kreuger J, Phillipson M. Identification and characterization of VEGF-A-responsive neutrophils expressing CD49d, VEGFR1, and CXCR4 in mice and humans. Blood. 2015 Oct 22;126(17):2016-26.
17 Katkoori VR, Basson MD, Bond VC, Manne U, Bumpers HL. Nef-M1, a peptide antagonist of CXCR4, inhibits tumor angiogenesis and epithelial‐to‐mesenchymal transition in colon and breast cancers. Oncotarget. 2015 Sep 29;6(29):27763-77.
18 Alatas F, Alatas O, Metintas M, Ozarslan A, Erginel S, Yildirim H. Vascular endothelial growth factor levels in active pulmonary tuberculosis. Chest. 2004 Jun;125(6):2156-9.
19 Tsai MC, Chakravarty S, Zhu G, Xu J, Tanaka K, Koch C, Tufariello J, Flynn J, Chan J. Characterization of the tuberculous granuloma in murine and human lungs: cellular composition and relative tissue oxygen tension. Cell Microbiol. 2006 Feb;8(2):218-32.
20 Matsuyama W, Hashiguchi T, Matsumuro K, Iwami F, Hirotsu Y, Kawabata M, Arimura K, Osame M. Increased serum level of vascular endothelial growth factor in pulmonary tuberculosis. Am J Respir Crit Care Med. 2000 Sep;162(3 Pt1):1120-2.
21 Saita N, Fujiwara N, Yano I, Soejima K, Kobayashi K. Trehalose 6,6'-dimycolate (cord factor) of Mycobacterium tuberculosis induces corneal angiogenesis in rats. Infect Immun. 2000 Oct;68(10):5991-7.
22 Oehlers SH, Cronan MR, Scott NR, Thomas MI, Okuda KS, Walton EM, Beerman RW, Crosier PS, Tobin DM. Interception of host angiogenic signalling limits mycobacterial growth. Nature. 2015 Jan 29;517(7536):612-5.
23 Ramakrishnan L. Revisiting the role of the granuloma in tuberculosis. Nat Rev Immunol. 2012 Apr 20;12(5):352-66.
24 Meijer AH. Protection and pathology in TB: learning from the zebrafish model. Semin Immunopathol. 2016 Mar;38(2):261-73.
25 Jin SW, Beis D, Mitchell T, Chen JN, Stainier DY. Cellular and molecular analyses of vascular tube and lumen formation in zebrafish. Development. 2005 Dec;132(23):5199-209.
26 Folkman J. Role of angiogenesis in tumor growth and metastasis. Semin Oncol. 2002 Dec;29(6 Suppl 16):15-8.
27 Li L, Jin H, Xu J, Shi Y, Wen Z. Irf8 regulates macrophage versus neutrophil fate during zebrafish primitive myelopoiesis. Blood. 2011 Jan 27;117(4):1359-69.
28 He S, Lamers GE, Beenakker JW, Cui C, Ghotra VP, Danen EH, Meijer AH, Spaink HP, Snaar-Jagalska BE. Neutrophil-mediated experimental metastasis is enhanced by VEGFR inhibition in a zebrafish xenograft model. J Pathol. 2012 Aug;227(4):431-45.
29 Triantafilou M, Lepper PM, Briault CD, Ahmed MA, Dmochowski JM, Schumann C, Triantafilou K. Chemokine receptor 4 (CXCR4) is part of the lipopolysaccharide "sensing apparatus". Eur J Immunol. 2008 Jan;38(1):192-203.
30 Kishore SP, Bungum MK, Platt JL, Brunn GJ. Selective suppression of Toll-like receptor 4 activation by chemokine receptor 4. FEBS Lett. 2005 Jan31;579(3):699-704.
31 Naldini A, Carraro F. Role of inflammatory mediators in angiogenesis. Curr Drug Targets Inflamm Allergy. 2005 Feb;4(1):3-8.
32 Jackson JR, Seed MP, Kircher CH, Willoughby DA, Winkler JD. The codependence of angiogenesis and chronic inflammation. FASEB J. 1997 May;11(6):457-65.
33 Carmi Y, Dotan S, Rider P, Kaplanov I, White MR, Baron R, Abutbul S, Huszar M, Dinarello CA, Apte RN, Voronov E. The role of IL-1β in the early tumor cell-induced angiogenic response. J Immunol. 2013 Apr 1;190(7):3500-9.
34 Nguyen-Chi M, Phan QT, Gonzalez C, Dubremetz JF, Levraud JP, Lutfalla G. Transient infection of the zebrafish notochord with E. coli induces chronic inflammation. Dis Model Mech. 2014 Jul;7(7):871-82.
35 Cha YR, Fujita M, Butler M, Isogai S, Kochhan E, Siekmann AF, Weinstein BM. Chemokine signaling directs trunk lymphatic network formation along the preexisting blood vasculature. Dev Cell. 2012 Apr 17;22(4):824-36.
36 Hudlicka O, Milkiewicz M, Cotter MA, Brown MD. Hypoxia and expression of VEGF-A protein in relation to capillary growth in electrically stimulated rat and rabbit skeletal muscles. Exp Physiol. 2002 May;87(3):373-81.

37 Stone J, Itin A, Alon T, Pe'er J, Gnessin H, Chan-Ling T, Keshet E. Development of retinal vasculature is mediated by hypoxia-induced vascular endothelial growth factor (VEGF) expression by neuroglia. J Neurosci. 1995 Jul;15(7 Pt 1):4738-47.
38 Datta M, Via LE, Kamoun WS, Liu C, Chen W, Seano G, Weiner DM, Schimel D, England K, Martin JD, Gao X, Xu L, Barry CE 3rd, Jain RK. Anti-vascular endothelial growth factor treatment normalizes tuberculosis granuloma vasculature and improves small molecule delivery. Proc Natl Acad Sci U S A. 2015 Feb 10;112(6):1827-32.
39 Azenshtein E, Meshel T, Shina S, Barak N, Keydar I, Ben-Baruch A. The angiogenic factors CXCL8 and VEGF in breast cancer: regulation by an array of pro-malignancy factors. Cancer Lett. 2005 Jan 10;217(1):73-86.
40 Heidemann J, Ogawa H, Dwinell MB, Rafiee P, Maaser C, Gockel HR, Otterson MF, Ota DM, Lugering N, Domschke W, Binion DG. Angiogenic effects of interleukin 8 (CXCL8) in human intestinal microvascular endothelial cells are mediated by CXCR2. J Biol Chem. 2003 Mar 7;278(10):8508-15.
41 Voronov E, Shouval DS, Krelin Y, Cagnano E, Benharroch D, Iwakura Y, Dinarello CA, Apte RN. IL-1 is required for tumor invasiveness and angiogenesis. Proc Natl Acad Sci U S A. 2003 Mar 4;100(5):2645-50.
42 Voronov E, Carmi Y, Apte RN. The role IL-1 in tumor-mediated angiogenesis. Front Physiol. 2014 Mar 28;5:114.
43 Schweighofer B, Testori J, Sturtzel C, Sattler S, Mayer H, Wagner O, Bilban M, Hofer E. The VEGF-induced transcriptional response comprises gene clusters at the crossroad of angiogenesis and inflammation. Thromb Haemost. 2009 Sep;102(3):544-54.
44 Torraca V, Otto NA, Tavakoli-Tameh A, Meijer AH, The inflammatory chemokine Cxcl18b exerts neutrophil-specific chemotaxis via the promiscuous chemokine receptor Cxcr2 in zebrafish. *Chapter 7 of this thesis.*
45 Tobin DM, Vary JC Jr, Ray JP, Walsh GS, Dunstan SJ, Bang ND, Hagge DA, Khadge S, King MC, Hawn TR, Moens CB, Ramakrishnan L. The lta4h locus modulates susceptibility to mycobacterial infection in zebrafish and humans. Cell. 2010 Mar 5;140(5):717-30.
46 Tobin DM, Roca FJ, Oh SF, McFarland R, Vickery TW, Ray JP, Ko DC, Zou Y, Bang ND, Chau TT, Vary JC, Hawn TR, Dunstan SJ, Farrar JJ, Thwaites GE, King MC, Serhan CN, Ramakrishnan L. Host genotype-specific therapies can optimize the inflammatory response to mycobacterial infections. Cell. 2012 Feb 3;148(3):434-46.
47 Roca FJ, Ramakrishnan L. TNF dually mediates resistance and susceptibility to mycobacteria via mitochondrial reactive oxygen species. Cell. 2013 Apr 25;153(3):521-34.
48 Bernut A, Herrmann JL, Kissa K, Dubremetz JF, Gaillard JL, Lutfalla G, Kremer L. Mycobacterium abscessus cording prevents phagocytosis and promotes abscess formation. Proc Natl Acad Sci U S A. 2014 Mar 11;111(10):E943-52.
49 Renshaw SA, Loynes CA, Trushell DM, Elworthy S, Ingham PW, Whyte MK. A transgenic zebrafish model of neutrophilic inflammation. Blood. 2006 Dec 15;108(13):3976-8.
50 van der Sar AM, Abdallah AM, Sparrius M, Reinders E, Vandenbroucke-Grauls CM, Bitter W. Mycobacterium marinum strains can be divided into two distinct types based on genetic diversity and virulence. Infect Immun. 2004 Nov;72(11):6306-12.
51 Takaki K, Davis JM, Winglee K, Ramakrishnan L. Evaluation of the pathogenesis and treatment of Mycobacterium marinum infection in zebrafish. Nat Protoc. 2013 Jun;8(6):1114-24.
52 Torraca V, Cui C, Boland R, Bebelman JP, van der Sar AM, Smit MJ, Siderius M, Spaink HP, Meijer AH. The CXCR3-CXCL11 signaling axis mediates macrophage recruitment and dissemination of mycobacterial infection. Dis Model Mech. 2015 Mar;8(3):253-69.
53 Benard EL, van der Sar AM, Ellett F, Lieschke GJ, Spaink HP, Meijer AH. Infection of zebrafish embryos with intracellular bacterial pathogens. J Vis Exp. 2012 Mar 15;(61).
54 Cui C, Benard EL, Kanwal Z, Stockhammer OW, van der Vaart M, Zakrzewska A, Spaink HP, Meijer AH. Infectious disease modeling and innate immune function in zebrafish embryos. Methods Cell Biol. 2011;105:273-308.
55 Rougeot J, Zakrzewska A, Kanwal Z, Jansen HJ, Spaink HP, Meijer AH. RNA sequencing of FACS-sorted immune cell populations from zebrafish infection models to identify cell specific responses to intracellular pathogens. Methods Mol Biol.2014;1197:261-74.